Injection molded lab-on-a-disc platform for screening of genetically modified E. coli using liquid-liquid extraction and surface enhanced Raman scattering

Morelli, Lidia; Serioli, Laura; Centorbi, Francesca Alessandra; Jendresen, Christian Bille; Matteucci, Marco; Ilchenko, Oleksii; Demarchi, Danilo; Nielsen, Alex Toftgaard; Zor, Kinga; Boisen, Anja

Published in:
Lab on a Chip

Link to article, DOI:
10.1039/c7lc01217a

Publication date:
2018

Document Version
Peer reviewed version

Injection molded lab on disc platform for screening of genetically modified *E. coli* using liquid-liquid extraction and surface enhanced Raman scattering

Lidia Morelli[a]*†, Laura Serioli[a]†, Francesca Alessandra Centorbi[c], Christian Bille Jendresen[b], Marco Matteucci[a], Oleksii Ilchenko[a], Danilo Demarchi[c], Alex Toftgaard Nielsen[b], Kinga Zór[a], Anja Boisen[a]

We present the development of an automated centrifugal microfluidic platform with integrated sample pre-treatment (filtration and liquid-liquid extraction) and detection (SERS-based sensing). The platform consists of eight calibration and four assay modules, fabricated with polypropylene using injection molding and bonded with ultrasonic welding. The platform was used for detection of a secondary bacterial metabolite (*p*-coumaric acid) from bacterial supernatant. The obtained extraction efficiency was comparable to values obtained in batch experiments and the SERS-based sensing showed a good correlation with HPLC analysis.

Introduction

Research in the field of metabolic engineering, related to the development of new microbial strains for sustainable production of valuable compounds, has increased significantly during the last decades. Screening of newly developed microorganisms, commonly performed using well-established, precise and accurate techniques, e.g. high performance liquid chromatography (HPLC),[1] is a crucial step in the development and optimization process in order to identify the best performing strains. The commonly used methods, in most cases, require complex, bulky instrumentation operated by skilled personnel, large quantities of solvents and reagents and are time and resource consuming. Reliable, cost and time-efficient, high-throughput, on-site detection would represent an ideal condition to overcome the limitations by the currently used approaches.[2]

In the screening process, selective detection is important when aiming for quantification of analytes produced by microorganisms. Raman scattering is increasingly used as a detection method in biological applications, due to the spectroscopic signal providing molecule-specific information about the sample, using little or no sample pre-treatment.[3,4] However, since not all molecules give a strong Raman signal, detection and quantification of small molecules in complex media are challenging, especially at low concentrations. Surface enhanced Raman scattering (SERS) is a well-established detection method for enhancing the signal of small molecules at low concentrations. Plasmonic enhancement of the incident electromagnetic field increases the Raman signal of several orders of magnitude, through the use of metallic nanostructured surfaces.[5] Due to its sensitivity and speed of detection, SERS-based sensing has been used for various application in microbiology, including detection of trace contaminants,[6] identification and discrimination of pathogens[7–10] or metabolomic profiling of bacterial supernatant.[11] On the other hand, reliable quantification with SERS can be challenging, due to the variability of laser performance as well as the instability and irreproducibility of commonly used SERS substrates. However, according to the literature[12,13] and based on our previous work,[14,15] quantification through SERS can be successfully achieved by using uniform and stable SERS substrates.[16,17]

p-Coumaric acid (pHCA) is a secondary bacterial metabolite, heterologously synthetized from tyrosine (Tyr) by *Escherichia coli* (*E. coli*) as a product of tyrosine ammonia-lyase (TAL) reaction.[1] It is a common precursor for many phenolic compounds, with several commercial applications.[18] Direct SERS detection of pHCA from bacterial supernatant proved to be challenging due to the complexity of the sample matrix.[19] Compounds, including Tyr, can interfere with pHCA detection due to overlapping vibrational peaks and/or preferential interaction with the SERS-active substrate. Furthermore, salts

[a] *Department of Micro- and Nanotechnology, Technical University of Denmark, 2800 Kgs. Lyngby, DENMARK.*
[b] *The Novo Nordisk Foundation Center for Biosustainability, Technical University of Denmark, 2800 Kgs. Lyngby, DENMARK.*
[c] *Department of Electronics and Telecommunications, Politecnico di Torino, 10129 Torino, ITALY.*
† The authors contributed equally to the presented work.
*e-mail: lmor@nanotech.dtu.dk, phone: +45 91 73 43 40
Electronic Supplementary Information (ESI) available: optimization of DCM/sample ratio, pure components detected in the standards used for calibration models and results of quantification using an incorrect calibration model. See DOI: 10.1039/x0xx00000x

from the bacterial culture medium accumulate on the active surface, significantly decreasing signal intensity.[19] We previously showed that a sample pre-treatment step using liquid-liquid extraction (LLE) can be combined with SERS-based sensing in order to improve the selectivity and sensitivity of the assay.[14]

Due to the need for real-time and high-throughput screening, several devices and microfluidic solutions[20–24] have been proposed and developed. Despite the small footprint of the developed microfluidic chips, in most cases fluidic platforms require complex actuation systems and fluidic handling solutions,[25,26] increasing the complexity and decreasing the usability and robustness of the setups. Centrifugal microfluidic platforms have emerged as advanced fluidic devices, able to overcome several limitations of conventional microfluidics.[27] Fluidic handling on the centrifugal platform is performed through a controlled spinning motor, eliminating the need for external pumps, tubes and connections. In addition, several microfluidic operations can be performed on the platform, such as valving, volume metering and mixing, enabling complex analysis on a small footprint. Lab-on-disc (LoD) devices have been developed and used for a wide range of applications, including diagnostics,[28] cell handling[29] and environmental analysis.[30] Furthermore, Kim *et al.* reported a centrifugal microfluidic platform for quantitative screening of microalgae based on sample pre-treatment and detection on disc.[31]

There are several reports presenting the integration of SERS-based sensing with fluidics[32] and microfluidics.[33,34] However, there is a limited number of papers about SERS sensing in LoD devices.[35,36] Furthermore, in some cases SERS detection on disc is based on nanoparticle aggregation, which can be more prone to reproducibility issues than SERS chips. Implementation of LLE on a LoD device has been reported either using external pumps[37] or organic solvents compatible with commonly used materials and fabrication processes.[31] The extraction of our target analyte required the use of an organic solvent, dichloromethane (DCM), which is not compatible with most common polymers, and therefore made the implementation of the presented LoD more challenging.

In this work we present the design and development of a centrifugal platform enabling detection of a secondary bacterial metabolite secreted by *E. coli* in supernatant, through sequential steps of filtration, LLE and SERS-based sensing. The challenges caused by the use of harsh chemicals were overcome by using a polypropylene (PP) microfluidic platform, which was fabricated through injection molding and sealed with ultrasonic welding.

Materials and methods

Chemicals, *E. coli* cultures and HPLC detection

100 mM pHCA stock solutions were freshly prepared in EtOH 99% and diluted in DCM for standards, and in bacterial growth medium and in control supernatant for characterization of the LLE assay. HCl 32% was used for acidification of samples and DCM was used as organic phase for LLE. Aqueous solutions were prepared with ultrapure water obtained from a Milli-Q purification system (Millipore Corporation, Billerica, MA, U.S.) and all the chemicals were purchased from Sigma-Aldrich (St. Louis, MO, USA).

E. coli strains CBJ786, CBJ951, CBJ789 and CBJ800, expressing TAL-encoding genes from IPTG-inducible promoters, were grown in M9 medium with 1% glucose, 2 mM tyrosine, 1 mM IPTG and antibiotics for maintenance of plasmids for 22 h as described in our previous work.[14] For quantification of pHCA in real samples, bacterial supernatant was obtained from each strain by centrifugation (10 min at 10000 *g*, 4 °C), and filtration through 0.2 µm filters and used on disc. Furthermore, in order to demonstrate the effectiveness of the filtration step on disc, bacterial aliquots from strain CBJ800 (OD_{600} = 10) were directly analyzed on disc without prior centrifugation.

Quantities of pHCA in samples were found by reversed-phase HPLC using separation on a HS-F5 column (Sigma-Aldrich) with previously described mobile phases (ammonium formate buffer and acetonitrile) and UV detection.[14]

SERS chip fabrication

The SERS substrates, consisting of gold-capped silicon nanopillars, were fabricated with the methods described by Wu et al.,[17] with 4 min etching time, followed by 1 min O_2 plasma cleaning and deposition of 220 nm Au at a rate of 10 Å/s. Wafers were diced with a Laser Micromachining tool (3D-Micromac AG, D-09126 Chemnitz, Germany) to fabricate 4x4 mm^2 chips for off-disc analysis and 2x4 mm^2 chips for integration on disc.

Fabrication and assembly of the centrifugal platform and integration of the SERS chip

The LoD device (Fig. 1 a)) consists of 12 fluidic units: four assay (Fig. 1 b)) and eight calibration modules (Fig. 1 c)), fixed on a poly(methyl methacrylate) (PMMA) disc with pressure sensitive adhesive (PSA) tape (ARcare 90106, Adhesive Research, Limerick, Ireland).

The filtration part in the assay module (Fig. 1 b), 1 - 6) was fabricated using 0.6 mm thick PMMA layers (Axxicon Moulds, Eindhoven, The Netherlands), laser ablated with an Epilog Mini 18 30 W system, from Epilog, USA. The PMMA layers were assembled with a 0.15 mm thick PSA tape, cut with a Silhouette Cameo Plotter (Silhouette America, Inc., Utah, US). In addition, the 6x6 mm^2 cellulose acetate membrane (Cellulose acetate circles (OE 66), 0.2 µm pores, Whatman™, Maidstone, United Kingdom) was embedded between two PSA

layers, enabling leak-proof filtration, as schematically shown in Fig. 2 d).

The assay (Fig. 1 b), 7 - 8) and the calibration module (Fig. 1 c)) were fabricated with clear PP (Borclear RF366MO, Borealis AG, Wien, Austria), a polymer used in a wide range of applications and resistant to most solvents, including DCM. The PP slides were injection molded (Victory Tech 80/45, Engel, Schwertberg, Austria) with 50 °C mold temperature (variotherm process), 750 bar holding pressure and 21 cm^3/s injection speed. The PP slides were then bonded with a Telsonic USP4700 20 kHz ultrasonic welder (Telsonic, Erlangen, Germany), with 100 J deposited during the welding, running at a 80% vibrational amplitude, with a holding time of 0.55 s and a down-pressure of 0.2 Pa (Fig. 2 f)). The SERS chip was immobilized in the sensing chamber with a double layer of PSA tape (Fig. 2 b)). The aluminum shim for injection molding was micromilled (Mini-Mill/3, Minitech Machinery Corp, GA, US) and 50 µm deep energy directors (Fig. 2 e)) were carved on the shim around the microfluidic features with a laser micromachining tool (3D-Micromac AG, D-09126 Chemnitz, Germany) to enable ultrasonic welding. Before welding, the hydrophilic siphons in the PP modules were wetted with Tween® 20 and dried for 1 h at 37 °C. The filtration part was fixed to the assay module with PSA tape and shortly pressed with a bonding press (PW 10 H, P/O/Weber, Germany) in order to maximize adhesion.

Microfluidic design

As described in our previous work,[14] sample pre-treatment is needed for SERS detection of pHCA in bacterial supernatant. The developed protocol,[14] previously performed manually, consists of a series of steps (supernatant filtration, acidification, mixing, addition of DCM, mixing, static incubation and SERS detection of pHCA in the extract).

We developed a LoD system with a custom microfluidic design in order to transfer all the sample pre-treatment steps on a centrifugal microfluidic platform (Fig. 2 c)). As a first step, the samples are placed in the loading chamber (1), followed by removal of bacterial cells in the filtration chamber (2). Since part of the sample is absorbed by the membrane, a metering chamber (3) and a siphon valve (4) are needed to meter a known sample volume (18 µL). An HCl loading chamber (5), a mixing chamber (6) and a serpentine siphon (7) enable acidification of the sample and optimal mixing. A DCM loading chamber (8) is connected to the top of an extraction chamber (9), where the aqueous and organic phase are mixed and incubated. The serpentine siphon is split into 4 microchannels at the bottom of the incubation chamber, in order to create bubbles and increase mixing efficiency. A sensing chamber, connected to the bottom of the extraction chamber, contains a 2x4 mm^2 SERS chip (10).

Besides the LLE assay module, a calibration module was also designed and fabricated, to enable detection of pHCA in DCM standards on the same LoD. As described in our previous work,[14] a calibration step is needed in order to perform quantification of bacterial pHCA. The microfluidic design, shown in Fig. 2 a), only includes a DCM loading chamber (1), an intermediate chamber (2), which minimizes unwanted DCM wetting of the SERS chip, and a sensing chamber (3) with the embedded SERS chip.

SERS data acquisition and analysis

When performing off-disc SERS sensing, 4x4 mm^2 SERS substrates were wet with 5 µL droplets and dried completely before acquisition. When performing SERS sensing on LoD, the disc was removed from the spinning motor immediately after the fluidic protocol and placed under the Raman microscope, in order to collect the signal on the dried SERS chip. SERS measurements were performed with a DXRxi Raman Imaging Microscope (Thermo Fisher Scientific Inc., Waltham, MA, US). The optical microscope is coupled to a spectrometer 5 cm^{-1} FWHM and ±2 cm^{-1} wavenumber accuracy. SERS spectra were collected at 780 nm with a laser power of 2 mW, 10x objective lens, 50 µm slit and 3.6 µm diameter estimated laser spot. Maps of 40 points with a 100 µm collection step were collected on the surface of each chip, and the spectrum collected in each point was averaged over 3 acquisitions of 0.05 s each.

Data pre-processing and quantitative analysis were performed with MatLab (version 8.4, MathWorks, Natick, MA, US) and TQ Analyst (version 9.2, Thermo Fisher Scientific Inc., Waltham, MA, US). An average SERS spectrum was obtained for each map after polynomial baseline correction (7^{th} order) and outlier removal, followed by the application of a partial least squares (PLS) algorithm for quantitative model building.

Standards with known concentrations were used to build the calibration models, and validation samples were randomly chosen for each concentration within the dataset in each case. The models were developed based on a first derivative algorithm in the wavenumber range 1080 - 1750 cm^{-1}, in conjunction with spectral smoothing (Savitzky – Golay, 7 points window, 4^{th} polynomial order).

Results and discussion

Optimization of DCM/sample ratio and integration of SERS chip on the LoD device

LLE is a well-established separation procedure for partition of an analyte between two immiscible phases, based on different affinity. In our previous work,[14] we performed LLE of pHCA from aqueous growth medium and bacterial supernatant samples to DCM as organic extraction phase, and subsequently analyzed the extracts through SERS. We demonstrated that this approach significantly increases the sensitivity and

selectivity of SERS sensing, enabling robust pHCA quantification.

In this work, experiments were performed according to the previously described methods,[14] in order to investigate the optimal DCM/sample ratio to be used on the LoD device. Briefly, samples of M9 medium spiked with 250 µM pHCA were acidified with HCl 32% at pH 0.15 and incubated with DCM for 30 min. Different DCM/sample ratios were analyzed in the range between 0.125 and 10. After incubation, 5 µL droplets of DCM were analyzed with SERS (Fig. S1). Signal intensity at 1169 cm^{-1}, previously chosen as the pHCA characteristic peak, was maximum at a DCM/sample ratio of 1. Therefore, this ratio was chosen for all the presented experiments on the developed LoD device.

Various approaches have been evaluated for the integration of a SERS substrate on the platform, such as mechanical clamping and immobilization using UV curable glue or double sided adhesive tape. We found that when the silicon chip was integrated through mechanical clamping, the energy in the welding process propagated through the chip through the clamping points resulting in broken SERS chip (not shown). Furthermore, when using liquid adhesives, such as UV curable glues, the chip surface was easily contaminated with glue, or the adhesive was not sufficient to prevent the chip from moving or breaking during welding. As shown in (Fig. 2 b)), the SERS chip was successfully integrated when fixed in the middle of the sensing chamber using double-sided tape.

Operation and flow control on the LoD platform

The fully integrated LLE/SERS microfluidic module was used for quantification of pHCA in spiked medium, supernatant samples and bacterial aliquots, according to the fluidic protocol summarized in Table 1. 25 µL sample was loaded, filtered through the membrane (Fig. 3 a)) and metered (Fig. 3 b)) at a rotational frequency of 60 Hz. After the excess sample flowed to the waste, a frequency of 1 Hz was set to prime the hydrophilic siphon (Fig. 3 c)). When the rotation of the LoD system was stopped, 1.8 µL HCl was loaded (Fig. 3 c)). At a frequency of 30 Hz, both HCl and the metered sample flowed in the mixing chamber, emptying the metering chamber (Fig. 3 d)). In the following step, the serpentine siphon was primed at 1 Hz (Fig. 3 e)) until the fluid reached the 4 microchannels at the bottom of the extraction chamber. The LoD device was then stopped and DCM was loaded (35 µl, Fig. 3 f)). The excess of loaded DCM was used to compensate for the fast evaporation during handling. A rotational frequency of 12.5 Hz was set to enable complete mixing between HCl and the sample through the serpentine siphon, and at the same time mixing between the acidified sample and DCM. During this step (Fig. 3 g)), DCM moved to the bottom of the chamber while the acidified sample moved to the top, forming bubbles and increasing the contact surface, due to the difference of density between phases. The phases were incubated for 5 minutes at a rotational frequency of 12.5 Hz, which was suitable to avoid any contact between DCM and the SERS substrate (Fig. 3 h)). After incubation, a rotational frequency of 50 Hz was set to wet the SERS chip for 5 s (Fig. 3 i). Since the detection chamber did not have any vent holes, the overpressure created at high speed pushed back the DCM level when decelerating. In fact, when setting a frequency of 1 Hz, DCM flowed back to the incubation chamber, letting the SERS chip dry (Fig. 3 j)). The excess sample was removed and the chip was ready for SERS acquisition. When performing calibration of DCM standards, only the steps 7, 9 and 10 were performed on the calibration module (Fig. 1 c)).

Table 1: Speed protocol for LLE and SERS wetting on disc. The acceleration was always set at 10 Hz^2.

Step	*Spinning speed*	*Time*	*Operation*	*Fluidic operation (Fig. 3)*
1	-	-	Sample loading	-
2	60 Hz	3 min	Sample filtration and metering	a), b)
3	1 Hz	5 s	Siphon priming	c)
4	-	-	HCl loading	c)
5	30 Hz	5	Sample acidification	d)
6	1 Hz	20 s	Serpentine siphon priming	e)
7	-	-	DCM loading	f)
8	12.5 Hz	5 min	Solvent mixing and incubation	g), h)
9	50 Hz	5 s	SERS chip wetting	i)
10	-	-	Excess sample removal and SERS acquisition	-

Quantification of M9 spiked samples

In order to evaluate the performance of the LLE/SERS LoD, we extracted and measured pHCA spiked in M9 medium at different concentrations. Based on our experiments we found that the extraction efficiency obtained with the LoD device (7.8 ± 1.1%) was comparable with the manually performed LLE previously validated by HPLC.[14] On Fig. 4 b), calculated concentrations were obtained using the extraction efficiency as follows:

$$calculated = \frac{detected \cdot 100}{\%\ extraction\ efficiency}$$

To enable quantification of pHCA in the samples, a calibration model was constructed, with the results shown in Fig. 4 a). For the calibration curve, 50 µL DCM standards between 0 and 80 µM were used and measured following the fluidic steps 7, 9 and 10 presented in Table 1. The PLS model proved to be

suitable for calibration and prediction of pHCA concentration (RMSEC = 1.82 µM, r^2 = 0.998 and RMSEP = 4.34 µM, r^2 = 0.994), with a detection limit (LOD) of 10 µM. By using the PLS model we were able to clearly separate the analyte signal from the effect of the background (Fig. S2).
Based on the presented calibration model and the calculated extraction efficiency, a good correlation was observed between expected and calculated values of pHCA in spiked M9 (Fig. 4 b)).

Screening of bacterial strains

A different calibration model was implemented for pHCA detection in supernatant samples than the one described for quantification in spiked M9 samples. We found that when using the calibration standards prepared in DCM, the model was not suitable for quantification of pHCA in real samples (Fig. S3). In order to improve the calibration model, we used a sample matrix that better mimicked bacterial samples, namely control supernatant (CBJ786). The control supernatant was obtained from a non-pHCA producing strain cultured in the same conditions as the producing ones. Known concentrations of pHCA (0, 250, 500, 750 µM) were spiked in the control supernatant, the samples were processed (LLE and SERS sensing) on the LoD and used to construct a calibration model using the PLS method (Fig. 5 a)).
When using the control supernatant as a sample matrix, the model proved to be suitable for calibration and quantification (RMSEC = 27.9 µM, r^2 = 0.995 and RMSEP = 51.9 µM, r^2 = 0.998, LOD = 100 µM; see also Fig. S4), and also in this case it was able to separate the analyte signal from the effect of background (Fig. S5). With this calibration model, we successfully quantified the pHCA content in real supernatant samples processed on LoD (Fig. S6), and we found a good correlation with HPLC results (Fig. 5b)).

Implementation of bacterial filtration on disc

When using SERS-based detection in complex matrices, the signal of the compound of interest can be significantly fouled. It was shown that salts and interfering molecules make direct sensing of pHCA in bacterial supernatant extremely challenging,[19] therefore there is a need for sample pre-treatment.[14,15] In the case of bacterial aliquots, the sample matrix is much more complex than bacterial supernatant due to the presence of *E. coli*, which can reach an OD_{600} up to 10 after 24 h culture.[38] Therefore, we investigated the influence of *E. coli* on LLE and SERS sensing on the developed platform and evaluated the effectiveness of the filtration unit, described in the Materials and Methods section.
One set of bacterial aliquots (CBJ800 at 24 h culture, OD_{600} = 10) was processed according to the complete protocol in Table 1, while others were loaded at the top of the metering chamber, skipping the filtration step. The SERS spectrum of the non-filtered bacterial aliquots (Fig. 6 a), black) showed lower signal intensity in the fingerprint region and no pHCA peak at 1169 cm^{-1} compared to filtered aliquots. Furthermore, when performing filtration prior to LLE and SERS detection, we obtained a clear peak for pHCA at 1169 cm^{-1} (Fig. 6 a), red) and found a good correlation with HPLC results (Fig. 6 b)).

Conclusions

We developed a centrifugal microfluidic platform with integrated sample pre-treatment and SERS-based detection. The functionality and usability of the device were proven by extracting a model secondary bacterial metabolite, pHCA, from culture medium, supernatant and bacterial aliquots. We found that LLE on LoD provides similar extraction efficiencies as the traditional batch extraction. By using a sample matrix similar to the real sample, we were able to develop a reliable method for quantification of pHCA in bacterial supernatant. Moreover, the integrated filtration enabled detection of pHCA directly from bacterial aliquots.
The presented LoD has a great potential for further automation and multiplexing, towards the development of an innovative high-throughput screening tool. The combination of a commonly used sample pre-treatment step (e.g. LLE) with a molecule-specific detection method (e.g. SERS) on a fluidic device can open up new possibilities for a wide range of applications (e.g. extraction and detection of other secondary metabolites in supernatant, such as antibiotics, vitamins and drugs) for industrial production and diagnostics.[39,40] Additionally, fabrication of the LoD through injection molding and ultrasonic welding opens up concrete possibilities for large scale production.

Conflicts of interest

There are no conflicts of interest to declare.

Acknowledgements

The research was funded by Danish National Research Foundation (DNRF122), Villum Fonden (Grant No. 9301), the European Research Council (320535, 'HERMES'). Christian Bille Jendresen was supported by The Novo Nordisk Foundation (Grant No. NNF15OC0015246).

References

1 C. B. Jendresen, S. G. Stahlhut, M. Li, P. Gaspar, S. Siedler, J. Förster, J. Maury, I. Borodina and A. T. Nielsen, *Appl. Environ. Microbiol.*, 2015, **81**, 4458–4476.
2 J. A. Dietrich, A. E. McKee and J. D. Keasling, *Annu. Rev. Biochem.*, 2010, **79**, 563–590.
3 H. J. Butler, L. Ashton, B. Bird, G. Cinque, K. Curtis, J. Dorney, K. Esmonde-White, N. J. Fullwood, B. Gardner, P. L.

Martin-Hirsch, M. J. Walsh, M. R. McAinsh, N. Stone and F. L. Martin, *Nat. Protoc.*, 2016, **11**, 664–687.
4 K. Klein, A. Gigler, T. Aschenbrenner, R. Monetti, W. Bunk, F. Jamitzky, G. Morfill, R. Stark and J. Schlegel, *Biophys. J.*, 2012, **102**, 360–368.
5 S. Nie, *Science*, 1997, **275**, 1102–1106.
6 K. Lee, T. J. Herrman, Y. Bisrat and S. C. Murray, *J. Agric. Food Chem.*, 2014, **62**, 4466–4474.
7 R. K. Lauridsen, T. Rindzevicius, S. Molin, H. K. Johansen, R. W. Berg, T. S. Alstrøm, K. Almdal, F. Larsen, M. S. Schmidt and A. Boisen, *Sens. Bio-Sensing Res.*, 2015, **5**, 84–89.
8 A. Walter, A. März, W. Schumacher, P. Rösch and J. Popp, *Lab Chip*, 2011, **11**, 1013.
9 A. Mühlig, T. Bocklitz, I. Labugger, S. Dees, S. Henk, E. Richter, S. Andres, M. Merker, S. Stöckel, K. Weber, D. Cialla-May and J. Popp, *Anal. Chem.*, 2016, **88**, 7998–8004.
10 A. März, B. Mönch, P. Rösch, M. Kiehntopf, T. Henkel and J. Popp, *Anal. Bioanal. Chem.*, 2011, **400**, 2755–2761.
11 W. R. Premasiri, J. C. Lee, A. Sauer-Budge, R. Théberge, C. E. Costello and L. D. Ziegler, *Anal. Bioanal. Chem.*, 2016, **408**, 4631–4647.
12 A. I. Radu, O. Ryabchykov, T. W. Bocklitz, U. Huebner, K. Weber, D. Cialla-May and J. Popp, *Analyst*, 2016, **141**, 4447–4455.
13 V. Peksa, M. Jahn, L. Štolcová, V. Schulz, J. Proška, M. Procházka, K. Weber, D. Cialla-May and J. Popp, *Anal. Chem.*, 2015, **87**, 2840–2844.
14 L. Morelli, K. Zór, C. B. Jendresen, T. Rindzevicius, M. S. Schmidt, A. T. Nielsen and A. Boisen, *Anal. Chem.*, 2017, **89**, 3981–3987.
15 L. Morelli, S. Z. Andreasen, C. B. Jendresen, A. T. Nielsen, J. Emnéus, K. Zór and A. Boisen, *Analyst*, 2017, **142**, 4553–4559.
16 M. S. Schmidt, J. Hübner and A. Boisen, *Adv. Mater.*, 2012, **24**, 11–18.
17 K. Wu, T. Rindzevicius, M. S. Schmidt, K. B. Mogensen, A. Hakonen and A. Boisen, *J. Phys. Chem. C*, 2015, **119**, 2053–2062.
18 Z. Lou, H. Wang, S. Rao, J. Sun, C. Ma and J. Li, *Food Control*, 2012, **25**, 550–554.
19 L. Morelli, C. B. Jendresen, K. Zor, T. Rindzevicius, M. S. Schmidt, A. T. Nielsen and A. Boisen, *Procedia Technol.*, 2017, **27**, 190–192.
20 R. Martínez and U. Schwaneberg, *Biol. Res.*, 2013, **46**, 395–405.
21 Y. Tang, M. Gan, Y. Xie, X. Li and L. Chen, *Lab Chip*, 2014, **14**, 1162.
22 B. L. Wang, A. Ghaderi, H. Zhou, J. Agresti, D. A. Weitz, G. R. Fink and G. Stephanopoulos, *Nat. Biotechnol.*, 2014, **32**, 473–8.
23 J. W. Lim, K. S. Shin, J. Moon, S. K. Lee and T. Kim, *Anal. Chem.*, 2016, **88**, 5234–5242.
24 H. S. Kim, T. L. Weiss, H. R. Thapa, T. P. Devarenne and A. Han, *Lab Chip*, 2014, **14**, 1415.
25 M. A. Kumar, M. A. Mazlomi, M. Hedström and B. Mattiasson, *Sensors Actuators B Chem.*, 2012, **161**, 855–861.
26 M. Mazlomi, M. Hedström and B. Mattiasson, *J. Biotechnol.*, 2010, **150**, 366–371.
27 O. Strohmeier, M. Keller, F. Schwemmer, S. Zehnle, D. Mark, F. von Stetten, R. Zengerle and N. Paust, *Chem. Soc. Rev.*, 2015.
28 R. Gorkin, J. Park, J. Siegrist, M. Amasia, B. S. Lee, J.-M. Park, J. Kim, H. Kim, M. Madou and Y.-K. Cho, *Lab Chip*, 2010, **10**, 1758–1773.
29 S. Hugo, K. Land, M. Madou and H. Kido, *S. Afr. J. Sci.*, 2014, **110**, 1–7.
30 D. A. Duford, Y. Xi and E. D. Salin, *Anal. Chem.*, 2013, **85**, 7834–7841.
31 Y. Kim, S.-N. Jeong, B. Kim, D.-P. Kim and Y.-K. Cho, *Anal. Chem.*, 2015, **87**, 7865–7871.
32 H.-Y. Wu and B. T. Cunningham, *Nanoscale*, 2014, 5162–5171.
33 Y. Deng, M. N. Idso, D. D. Galvan and Q. Yu, *Anal. Chim. Acta*, 2015, **863**, 41–48.
34 J. Leem, H. W. Kang, S. H. Ko and H. J. Sung, *Nanoscale*, 2014, **6**, 2895.
35 D. Choi, T. Kang, H. Cho, Y. Choi and L. P. Lee, *Lab Chip*, 2009, **9**, 239–43.
36 O. Durucan, T. Rindzevicius, M. S. Schmidt, M. Matteucci and A. Boisen, *ACS Sensors*, 2017.
37 A. Kazarine, M. C. R. Kong, E. J. Templeton and E. D. Salin, *Anal. Chem.*, 2012, **84**, 6939–6943.
38 K. Sanger, K. Zór, C. Bille Jendresen, A. Heiskanen, L. Amato, A. Toftgaard Nielsen and A. Boisen, *Sensors Actuators, B Chem.*, 2017, **253**, 999–1005.
39 N. E. Markina, V. V. Shalabay, A. M. Zakharevich and A. V. Markin, in *Proc. SPIE 9917, Saratov Fall Meeting 2015: Third International Symposium on Optics and Biophotonics and Seventh Finnish-Russian Photonics and Laser Symposium (PALS)*, 2016, vol. 9917, p. 99170X–1–5.
40 V. V. Shalabay, N. E. Markina, V. V. Galushka, A. M. Zakharevich, A. V. Markin and I. Y. Goryacheva, in *Progress in Biomedical Optics and Imaging - Proceedings of SPIE*, 2017, vol. 10336, pp. 1033613-1–6.

Figures

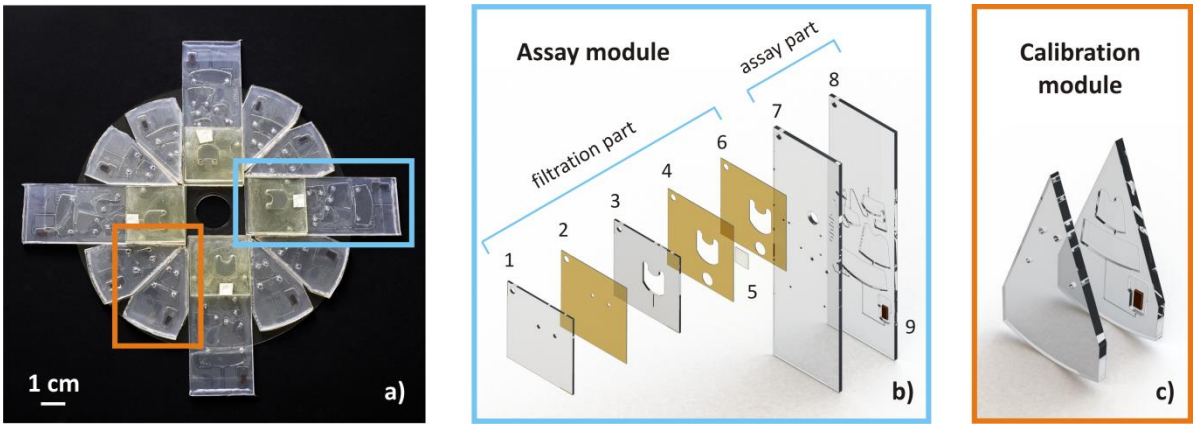

Fig. 1 a) Lab-on-a-disc for LLE extraction and detection of bacterial metabolites. The LoD device is composed of 12 modules on a PMMA disc. b) Exploded view of the assay module with the filtration part (1-6) containing a cellulose acetate membrane (5) and the assay part (7-9), with an embedded SERS chip (9). c) Exploded view of the calibration module with SERS chip.

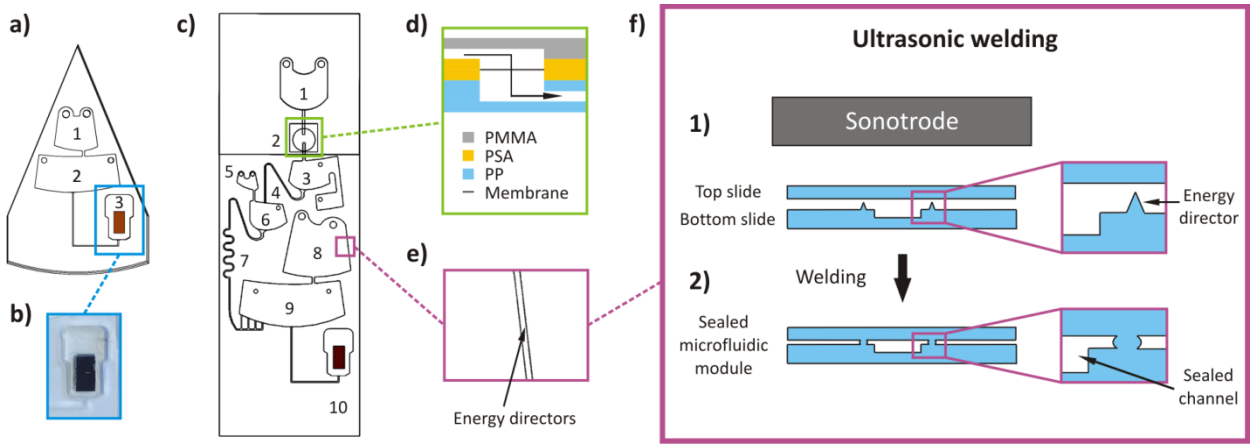

Fig. 2 a) Fluidic design of the calibration module, composed of a DCM loading (1), an intermediate (2) and a sensing chamber (3), where a SERS chip is immobilized with PSA tape. c) Microfluidic design of the assay module, composed of a loading (1), a filtration (2) and a metering chamber (3) and a hydrophilic siphon (4). The HCl loading chamber (5) is connected to the mixing chamber (6) followed by a serpentine siphon (7) enabling efficient mixing. The DCM loading chamber (8) is connected to the serpentine siphon through the extraction chamber (9), which is directly communicating with the detection chamber (10). d) Schematics of the filtration chamber, showing the integration of the cellulose acetate membrane between PSA layers and the direction of the flow. e) Representation of energy directors at the edge of a microfluidic chamber. f) Schematic representation of the working principle of ultrasonic welding, including a sketch of energy directors before (1) and after (2) welding.

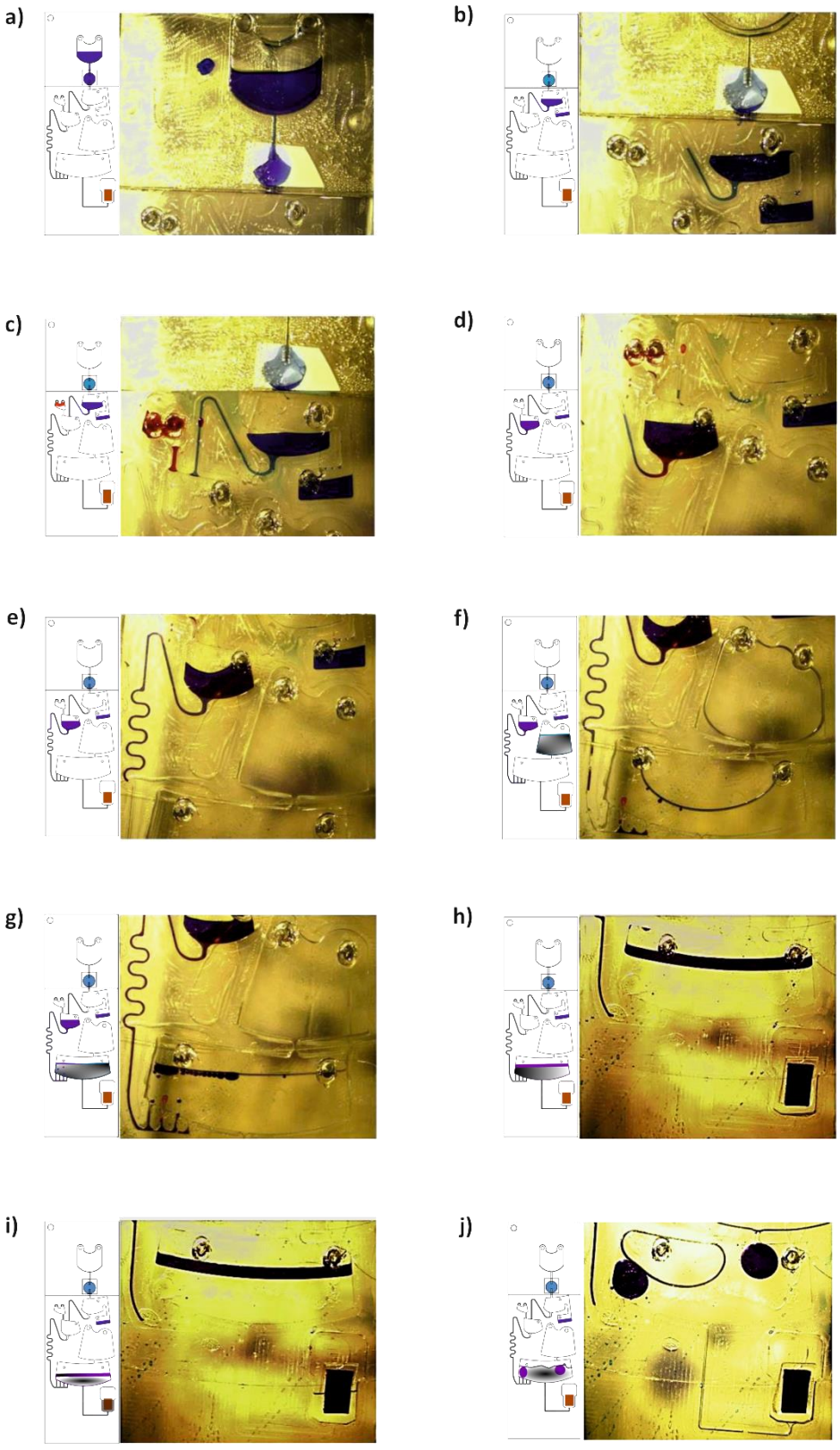

Fig. 3 Schematic representation of the lab-on-a-disc operation steps, and corresponding images captured from a video recorded with a CCD camera. a) Filtration of the sample (blue dye) and b) metering. c) Loading of HCl (red dye) and d) mixing of sample and HCl. e) Priming of serpentine siphon followed by f) loading of DCM (transparent). g) Bubble formation during phase mixing and h) incubation. i) Wetting of the SERS chip and j) emptying of the sensing chamber. For better visualization, in this experiment the DCM/sample ratio was increased to 3.

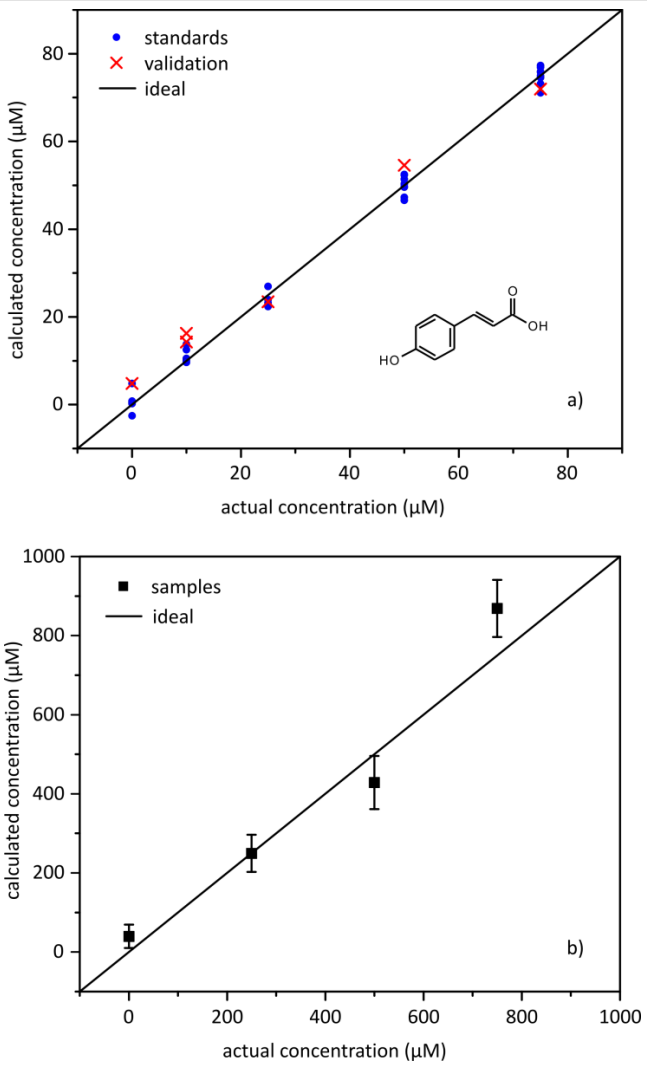

Fig. 4 a) A PLS model for pHCA amount prediction, based on spiked DCM standards. Triplicates were performed for each concentration, and 2 maps were collected from each chip (n = 6). Among these, samples marked with (x) were used for model validation. b) Correlation between actual and calculated pHCA concentration in spiked M9 medium after being processed on the LoD device. Each point is the average of triplicate chips, with 2 maps collected from each chip (n = 6).

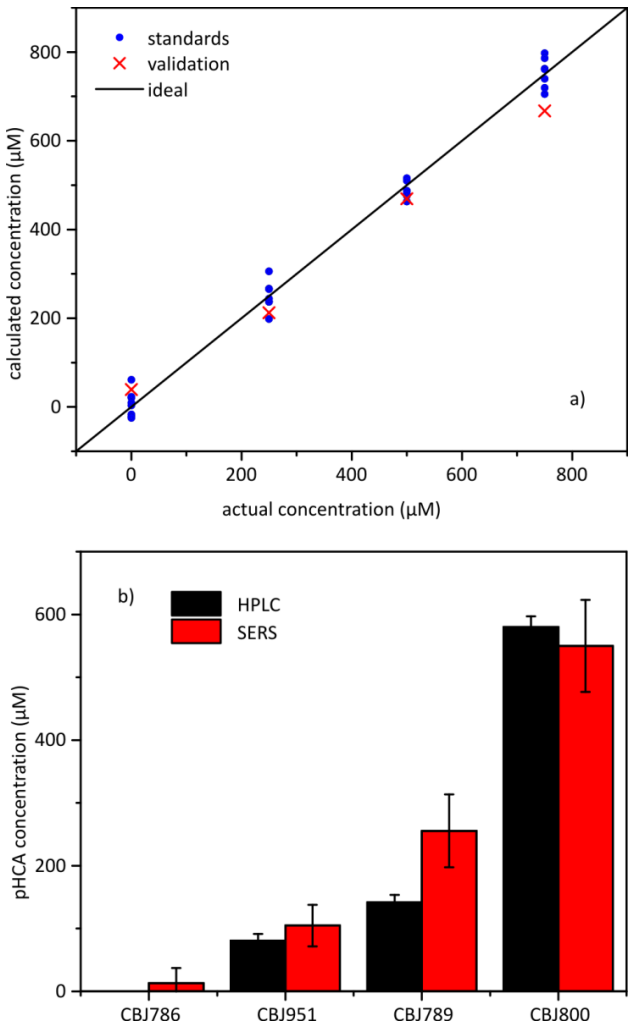

Fig. 5 a) A PLS model for pHCA amount prediction, based on spiked control supernatant processed on the LoD device. Triplicates were performed for each concentration, and 2 maps were collected from each chip (n = 6). Among these, samples marked with (x) were used for model validation. b) Quantification of pHCA in supernatant samples on the LoD system and comparison with HPLC data. Each SERS point is the average of triplicate chips, with 2 maps collected from each chip (n = 6). Each HPLC point is the average of triplicate injections (n = 3).

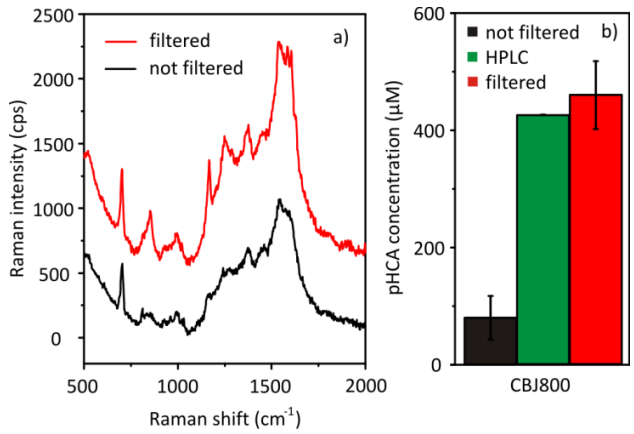

Fig. 6 a) SERS spectra of filtered and not filtered bacterial aliquots, processed on the LoD system. Each spectrum is the average of a 48-points map. b) Quantitative comparison between filtered and not filtered bacterial aliquots vs. HPLC data. Each SERS point is the average of triplicates, with 2 maps collected from each chip (n = 6). The HPLC point is the average of triplicate injections.

Supporting Information:

Injection molded lab on disc platform for screening of genetically modified E. coli using liquid-liquid extraction and surface enhanced Raman scattering

Lidia Morelli[a]*†, Laura Serioli[a]†, Francesca Alessandra Centorbi[c], Christian Bille Jendresen[b], Marco Matteucci[a], Oleksii Ilchenko[a], Danilo Demarchi[c], Alex Toftgaard Nielsen[b], Kinga Zór[a], Anja Boisen[a]

[a] *Department of Micro- and Nanotechnology, Technical University of Denmark, 2800 Kgs. Lyngby, DENMARK.*
[b] *The Novo Nordisk Foundation Center for Biosustainability, Technical University of Denmark, 2800 Kgs. Lyngby, DENMARK.*
[c] *Department of Electronics and Telecommunications, Politecnico di Torino, 10129 Torino, ITALY*

**e-mail: lmor@nanotech.dtu.dk, phone: +45 91 73 43 40*
† The authors contributed equally to the presented work.

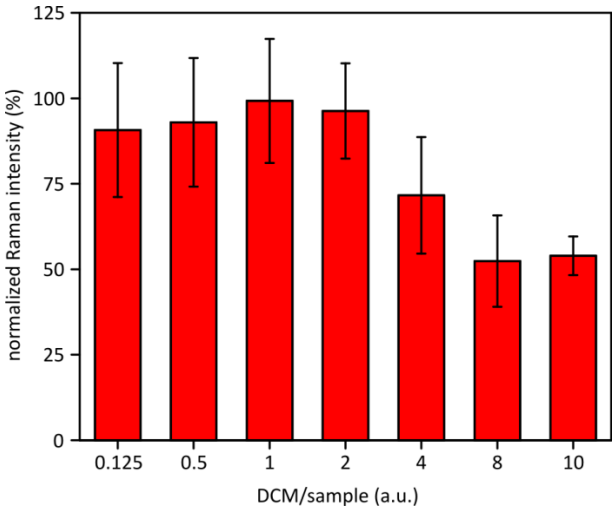

Fig. S1 Normalized Raman intensity at 1169 cm^{-1} for various DCM/sample ratios. Each ratio was tested on 2 SERS substrates, and 3 maps of 48 points were collected from each chip (n = 6), with error bars representing standard deviation. Intensities were normalized by the maximum value obtained.

When applying the PLS model to spiked DCM samples, the analysis of pure components showed that the analyte spectrum (Fig. S2 a)) closely resembled SERS fingerprint of pHCA, detected through SERS in our previous works.[1,2] Therefore, the model was able to isolate the contribution of pHCA from the background (Fig. S2 b)), and enabled good quantification.

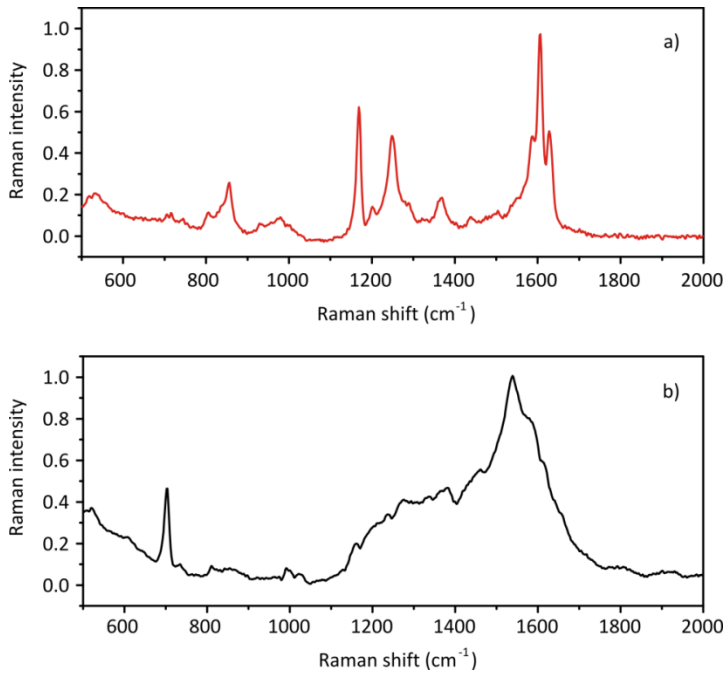

Fig. S2 Graphs of pure components detected in spiked DCM. a) Analyte component and b) background component.

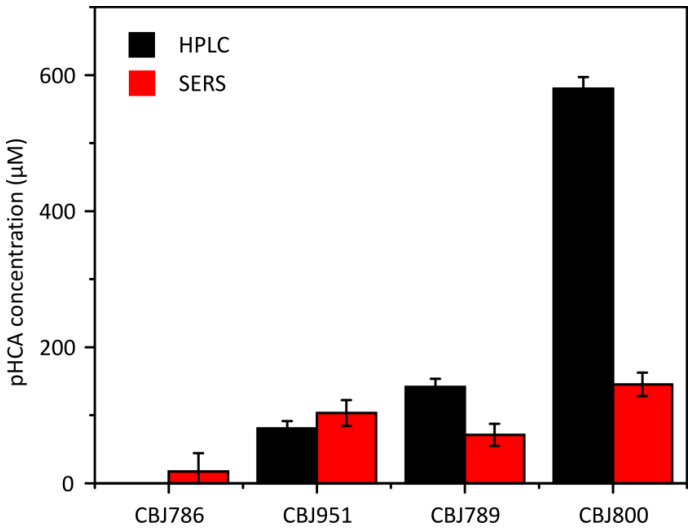

Fig. S3 Quantification of pHCA in supernatant using a calibration model based on spiked DCM standards. Each SERS point is the average of triplicate chips, with 2 maps collected from each chip (n = 6). Each HPLC point is the average of triplicate injections (n = 3).

The number of factors used for the spiked supernatant calibration model was chosen based on the predicted residual error sum of squares (PRESS), calculated through the TQ Analyst software and represented in Fig. S4. The suggested number of factors to avoid overfitting was three, corresponding to the minimum PRESS value in the graph.

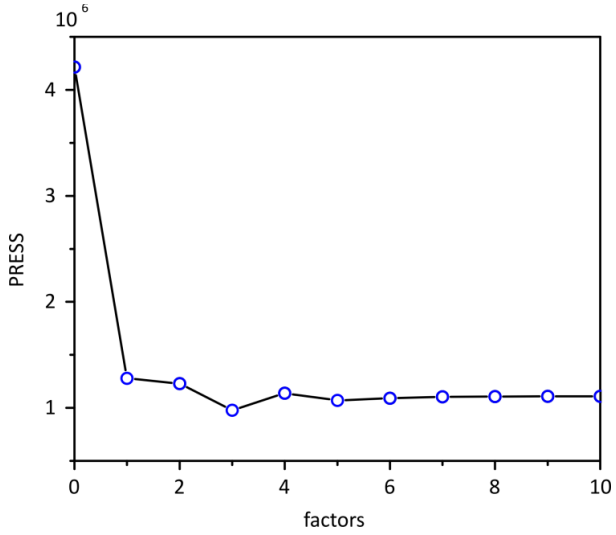

Fig. S4 The predicted residual error sum of squares (PRESS) for the spiked supernatant calibration model.

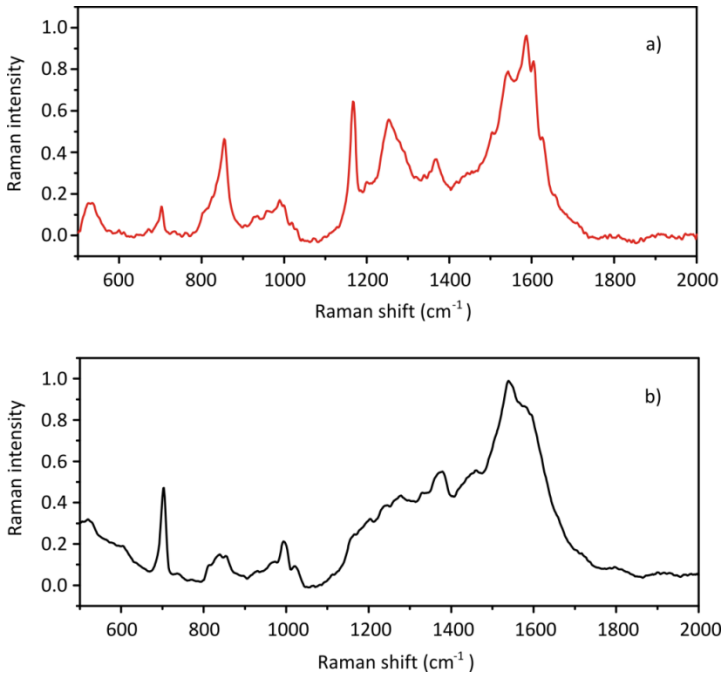

Fig. S5 Graphs of pure components detected in spiked supernatant (CBJ786). a) Analyte component and b) background component.

Fig. S6 shows the mean spectra and standard variations of each bacterial strain in the spectral region used for the PLS model. Since all the spectra share the same peak positions and band intensity variations, the SERS measurements were considered suitable for pHCA quantification.

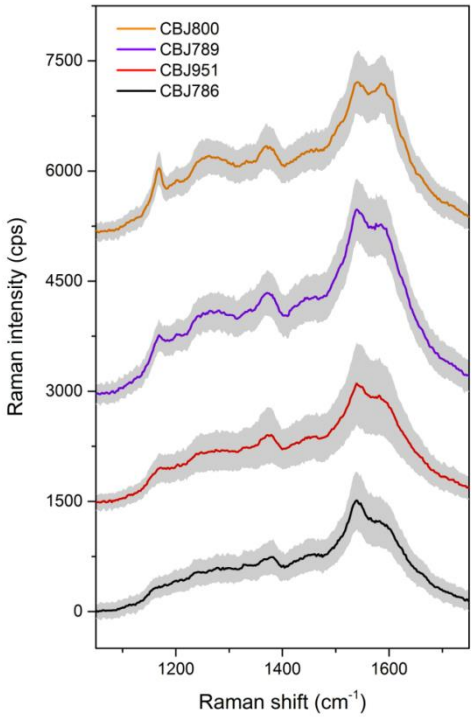

Fig. S6 Mean SERS spectra of *E. coli* samples collected on disc after data pre-processing, with the distribution of all individual spectra (n = 240) represented by the standard deviation in a grey shade.

References

1 L. Morelli, K. Zór, C. B. Jendresen, T. Rindzevicius, M. S. Schmidt, A. T. Nielsen and A. Boisen, *Anal. Chem.*, 2017, **89**, 3981–3987.

2 L. Morelli, S. Z. Andreasen, C. B. Jendresen, A. T. Nielsen, J. Emneus, K. Zor and A. Boisen, *Analyst*, 2017.